



# 1 Approaches to radar reflectivity bias correction to improve 2 rainfall estimation in Korea

3

4 C.-H. You<sup>1</sup>, M.-Y. Kang<sup>2</sup>, D.-I. Lee<sup>1,2</sup>, and J.-T., Lee<sup>2</sup>

5 [1] {Atmospheric Environmental Research Institute, Pukyong National University, Busan,  
6 South Korea }

7 [2] {Department of Environmental Atmospheric Sciences, Pukyong National University,  
8 Busan, South Korea }

9 Correspondence to: D.-I. Lee (leedi@pknu.ac.kr)

10

## 11 Abstract

12 Three methods for determining the reflectivity bias of single polarization radar using dual  
13 polarization radar reflectivity and disdrometer data (i.e., the equidistance line, overlapping  
14 area, and disdrometer methods) are proposed and evaluated for two low-pressure rainfall  
15 events that occurred over the Korean Peninsula on 25 August 2014 and 8 September 2012.  
16 Single polarization radar reflectivity was underestimated by more than 12 dB and 7 dB in the  
17 two rain events, respectively. All methods improved the accuracy of rainfall estimation,  
18 except for one case where DSDs were not observed, as the precipitation system did not pass  
19 through the disdrometer location. The use of these bias correction methods reduced the RMSE  
20 by as much as 50%. Overall, the most accurate rainfall estimates were obtained using the  
21 overlapping area method to correct radar reflectivity. A combination of all three methods  
22 would produce more accurate rainfall estimates, provided optimal values are determined for  
23 the domain size for the overlapping area method, the sample number threshold for the  
24 equidistance line method, and the reflectivity threshold for the disdrometer method.

25

## 26 1 Introduction

27 Radar is a useful remote sensing instrument for measuring rainfall amount, due to its  
28 relatively high resolution in both space and time. Rainfall rate is not measured directly, but  
29 must be derived from radar reflectivity. This derivation of radar rainfall is based on the



1 relationship between reflectivity ( $Z$ ) and rainfall rate ( $R$ ), known as the  $Z$ - $R$  relation ( $R(Z)$ ).  
2 Experimentally measured drop size distributions (DSDs) have been used extensively to obtain  
3 both radar reflectivity and rainfall rate (Compos and Zawadzki, 2000; Jang et al., 2004; You  
4 et al., 2004). There does not be existed a unique  $R(Z)$ , since DSDs can vary between storms  
5 and even within a single storm (Battan 1973; You et al., 2010).

6 However, radar rainfall estimation is complicated by a number of uncertainties including  
7 hardware calibration, partial beam filling, rain attenuation, brightband, and non-weather  
8 echoes (Wilson and Brandes, 1979; Austin, 1987). The correction of bias in  $Z$  caused by  
9 hardware calibration error is difficult to achieve using single polarimetric radar (SPOL) alone.  
10 Polarimetric radar (DPOL) provides a new method for the absolute calibration of reflectivity,  
11 which has been a longstanding problem with single polarization radar data. The method is  
12 based on the assumptions that  $Z$ , differential reflectivity ( $Z_{DR}$ ), and specific differential phase  
13 ( $K_{DP}$ ) are independent of each other, and that  $Z$  can be estimated from  $Z_{DR}$  and  $K_{DP}$ , which are  
14 insensitive to radar miscalibration (Gorgucci et al., 1992, 1999; Goddard et al., 1994;  
15 Sarchilli et al., 1996; Vivekanandan et al., 1999).

16 The Korea Meteorological Administration (KMA) is in the process of replacing Doppler  
17 radars with S-band DPOLs (to be completed by 2019), and Ministry of Land, Infrastructure  
18 and Transport (MoLIT) has installed four S-band DPOLs for operational use since 2009. Until  
19 the DPOL installation is complete, it is necessary to use a combination of SPOLs and DPOLs  
20 to produce rainfall mosaics covering the whole Korean Peninsula. To obtain more accurate  
21 mosaicked radar rainfall, SPOL reflectivity should be corrected using the reflectivity of  
22 DPOLs and other instruments such as disdrometer. Accurate SPOL reflectivity is also  
23 required for climatological analysis using radar rainfall.

24 This paper discusses three methods for reducing errors in SPOL reflectivity using DPOL and  
25 DSD measurements. In Section 2, the dataset used for the analysis is introduced, and three  
26 approaches to correcting SPOL reflectivity are described, along with methods for bias  
27 correction of DPOL reflectivity and  $Z_{DR}$ , and for validation. In Section 3, the results obtained  
28 using the three correction methods are compared with gauge measurements. Finally, we  
29 summarize the results and provide conclusions in Section 4.

30



## 1 **2 Data and methodology**

### 2 **2.1 Gauge, disdrometer, and radar datasets**

3 Rainfall data from rain gauges operated by the KMA were used to evaluate the accuracy of  
4 radar rainfall. Rain gauges located between 5 and 134 km from the radar were included in the  
5 analysis. Figure 1 shows the location of all instruments used in this study. The PARSIVEL  
6 (PARTicle SIZE VELOCITY) disdrometer was installed ~9 km from PSN. PARSIVEL is a laser-  
7 optic system that measures 32 channels from 0.062 to 24.5 mm (for detailed specifications,  
8 see Löffler-Mang and Joss, 2000).

9 Data were regarded as unreliable and removed from the analysis in the case that any of the  
10 following conditions were met: 1 min rain rate was less than  $0.1 \text{ mm h}^{-1}$ ; total number  
11 concentration from all channels was less than 10; drop numbers were recorded only in the  
12 lower 10 channels (1.187 mm for PARSIVEL); or drop numbers were recorded only in the  
13 lower 5 channels (0.562 mm for PARSIVEL) (You et al., 2015).

14 Radar data were recorded at PSN and BSL, which were installed and are operated by KMA  
15 and MoLIT, respectively. The transmitted peak power of BSL is 750 kW, the beam width is  
16  $0.95^\circ$ , the frequency is 2.791 GHz, and the antenna is 1085 m above sea level. The  
17 polarimetric variables are estimated with a gate size of 0.125 km. The scan strategy consists  
18 of six elevation angles with a 2.5 min update interval. The transmitted peak power of PSN is  
19 800 kW, the beam width is 1.0 degrees, and the antenna is 547 m above sea level. The  
20 reflectivity is estimated with a gate size of 0.25 km. The PSN scan strategy consists of 13  
21 elevation angles with a 10 min update interval. Radar variables at an elevation angle of 0.5  
22 (1.8) degrees were extracted from the BSL (PSN) data every 10 mins, to match the time  
23 interval for this study. Non-meteorological targets were removed from the PSN data using the  
24 texture and vertical gradient of reflectivity, as proposed by Zhang et al. (2004). Polarimetric  
25 variables were subjected to quality control using a threshold of 15 degrees for the standard  
26 deviation of the differential phase shift (You et al., 2014).

### 27 **2.2 Methodology for bias correction of PSN reflectivity**

28 To calculate the reflectivity bias of PSN, which is single polarization radar, three approaches  
29 were used: the equidistance line method, the overlapping area method, and the disdrometer  
30 method. The first approach is to compare the reflectivities along the line that is equidistant



1 between the two radars. To determine this line for the two radars, the effective radius was set  
2 to 100 km and the distance between the two radars and the azimuthal angle pointing from  
3 BSL to PSN were calculated using their latitude and longitude values. The start and end  
4 azimuthal angles for comparison of reflectivity were then calculated as follows:

$$5 \quad AZ_{st} = \beta - a \cos(0.5 \times dr / rc) \quad (1)$$

$$6 \quad AZ_{end} = \beta - a \cos(0.5 \times dr / rc) + 2 \times a \cos(0.5 \times dr / rc), \quad (2)$$

7 where  $AZ_{st}$  and  $AZ_{end}$  are the start and end azimuthal angles for the comparison, respectively;  
8  $\beta$  is an azimuthal angle which is the angle between north and the bearing from BSL points to  
9 PSN and  $rc$  and  $dr$  are the effective radius and distance from BSL to PSN, respectively. The  
10 distance between the two radars is 76.9 km, and the start and end azimuthal angles of DPOL  
11 (SPOL) are 79 (35) and 213 (261) degrees, respectively (Fig. 2).

12 To compare the reflectivity observed of targets at similar heights from both radars, the beam  
13 height was calculated assuming a standard atmospheric beam propagation (Rinehart, 2010), as  
14 follows:

$$15 \quad H = \sqrt{r^2 + (R' + H_0)^2} + 2r(R' + H_0) \sin \phi - R', \quad (3)$$

16 where  $r$  is the slant range from the radar,  $\phi$  is the elevation angle of the radar beam,  $H_0$  is the  
17 height of the radar antenna above sea level, and  $R' = (4/3)R$ , where  $R$  is the Earth's radius  
18 (6,371 km). The radar antenna heights of SPOL and DPOL are 547 and 1085 m, respectively.  
19 Figure 3 shows the beam height of PSN and BSL at the equidistance line. EL1 to EL6 show  
20 the elevation angles from smallest to largest. The smallest difference in beam height between  
21 the two radars is 149 m, which was obtained using the fourth elevation angle of PSN and the  
22 third elevation angle of BSL.

23 In the second approach, the overlapping area for the two radars was calculated by  
24 matching the coordinates. The polar coordinate of two radars was converted to a Cartesian  
25 coordinate with a spatial resolution of 1 km. The overlapping area was then determined by  
26 multiplying the distances between the two radars in the east–west and north–south directions.  
27 Figure 4 shows a schematic diagram of the overlapping area for the two radars. The extracted  
28 domain of PSN and BSL for the comparison is  $158 \times 136$  km.



1 The third and final approach is to use DSD observations from the PARSIVEL disdrometer.  
2 The reflectivity was calculated from the DSD measurements at 1 min resolution, and averaged  
3 over 10 mins to match the radar time resolution. Figure 5 shows a schematic of the procedure  
4 used to match the radar and PARSIVEL data. The PARSIVEL disdrometer is located ~9 km  
5 from the radar, at an azimuthal angle of 87 degrees. The radar reflectivity was averaged over a  
6 domain of 13 gates  $\times$  3 degrees in azimuth, centered at the PARSIVEL location.

### 7 **2.3 Z and $Z_{DR}$ bias correction for BSL**

8 Before calculating reflectivity bias for PSN using BSL, reflectivity and  $Z_{DR}$  must be corrected  
9 for systematic bias.  $Z_{DR}$  bias correction is important for the absolute calibration of the radar  
10 using a self-consistency method. Gorgucci et al. (1999) proposed using a vertical pointing  
11 scan of light rain, to take advantage of the nearly spherical shape of the raindrops as seen  
12 from below. Ryzhkov et al (2005) used the elevation angle dependency of  $Z_{DR}$  as an  
13 alternative technique and concluded that the high variability of  $Z_{DR}$  in rainfall prohibited the  
14 method from achieving the required absolute calibration accuracy of 0.2 dB. They instead  
15 proposed a method that utilizes the structural characteristics of the melting layer in stratiform  
16 clouds and the dry aggregated snow present above the melting layer.  $Z_{DR}$  measurements from  
17 dry aggregated snow above the melting layer resulted in a mean S-band value of 0.2 dB and  
18 an accuracy of 0.1–0.2 dB. Trabal et al. (2009) evaluated two methods using the intrinsic  
19 properties of dry aggregated snow present above the melting layer and light rain  
20 measurements close to the ground, and found that a  $Z_{DR}$  calibration accuracy of 0.2 dB or  
21 better was achieved using either method.

22 Vertical pointing data were not available in the present case, and the scan strategy, with six  
23 elevation angles, was unable to detect the melting layer. Therefore, in this study, light rain  
24 measurements close to the ground were used to calibrate  $Z_{DR}$  and reflectivity using a self-  
25 consistency method. Light rain was defined using a threshold of  $20 \text{ dBZ} \leq Z \leq 28 \text{ dBZ}$ , as  
26 proposed by Marks et al. (2011). The  $Z_H$  bias was calculated following the method of  
27 Ryzhkov et al. (2005), using a 9-gate moving average of  $Z_{DR}$  to improve the accuracy.



## 1 2.4 Validation

2 The normalized error (NE), root-mean-square error (RMSE), and correlation coefficient (CC)  
3 between rainfall estimates and measurements from 121 gauges were calculated to measure the  
4 performance of each bias correction method. These quantities are defined as follows:

$$5 \quad NE = \frac{\frac{1}{N} \sum_{i=1}^N |R_{R,i} - R_{G,i}|}{\overline{R_G}} \quad (3)$$

$$6 \quad RMSE = \left[ \frac{1}{N} \sum_{i=1}^N (R_{R,i} - R_{G,i})^2 \right]^{1/2} \quad (4)$$

$$7 \quad CC = \frac{\sum_{i=1}^N (R_{R,i} - \overline{R_R})(R_{G,i} - \overline{R_G})}{\left[ \sum_{i=1}^N (R_{R,i} - \overline{R_R})^2 \right]^{1/2} \left[ \sum_{i=1}^N (R_{G,i} - \overline{R_G})^2 \right]^{1/2}}, \quad (5)$$

8 where N is the number of radar rainfall ( $R_R$ ) and gauge rainfall ( $R_G$ ) pairs, and  $\overline{R_R}$  and  $\overline{R_G}$  are  
9 the average hourly rain rates from radar and gauges, respectively. These quantities were  
10 calculated using 1 hour rainfall amounts from radar and gauge measurements at each point.  
11 The radar rainfall value at each point was obtained by averaging rainfall over a small area (1  
12 km × 1°) centered on the corresponding rain gauge. The radar rainfall was calculated using  
13 the relation  $Z = 200 R^{1.6}$ .

14

## 15 3 Results

16 The accuracy of rainfall estimation using corrected reflectivity was evaluated to measure the  
17 effectiveness of each method for calculating reflectivity bias. Two rainfall events were used,  
18 occurring on 25 August 2014 and 8 September 2012 (Table 1). The August and September  
19 events were caused by low pressure systems over southern and northern Korea, respectively.

### 20 3.1 Equidistance line method

21 Before estimating radar rainfall rates, reflectivity biases were calculated using each of the  
22 three methods. Figure 6 shows time series of the average reflectivity difference between PSN  
23 and BSL at the equidistance line and the number of samples used in each calculation, on 25



1 August 2014. The average difference over the entire time period was  $-7.85$  dB, and the largest  
2 difference was  $-12.46$  dB. The number of samples used for each calculation was determined  
3 using a beam height difference threshold of  $0.1$  km. The total number of the samples  
4 satisfying the threshold along the equidistance line was  $77$ . The number of samples was  
5 generally above  $40$ , but it was smaller than  $40$  at  $1120$  LST and after  $1500$  LST. Figure 7  
6 shows the same information for 8 September 2012. The average reflectivity difference over  
7 the entire time period was  $-2.56$  dB, and the largest difference was  $-6.77$  dB. The number of  
8 samples was less than  $50$  until  $0310$  LST, after which it increased to more than  $60$ . This result  
9 suggests that the precipitation system was not located over the equidistance line until  $0310$   
10 LST.

11 Figure 8 shows the scatter plot of 1 hour radar rainfall, calculated using  $Z = 200 R^{1.6}$ , and  
12 gauge rainfall, for 25 August 2014 and 8 September 2012. The RMSE, NE, and CC for  
13 rainfall pairs on 25 August 2014 were improved from  $65.7$  to  $32.6$  mm, from  $0.79$  to  $0.36$ , and  
14 from  $0.88$  to  $0.89$ , respectively. On 8 September 2012, the RMSE, NE, and CC changed from  
15  $30.0$  to  $22.5$  mm, from  $0.58$  to  $0.41$ , and from  $0.81$  to  $0.78$ , respectively, by the use of bias  
16 correction. In both cases, the use of corrected reflectivity for rainfall estimation resulted in  
17 much better accuracy than did using raw reflectivity.

### 18 **3.2 Overlapping area method**

19 Figure 9 shows time series of the mean reflectivity differences between PSN and BSL in the  
20 overlapping area, and the number of samples used in each calculation (black squares) on 25  
21 August 2014. Bias values ranged from  $-11.7$  to  $-8.3$  dB over the period analyzed. The bias  
22 was stable until  $1440$  LST, after which it fluctuated as the number of samples decreased.  
23 Figure 10 shows the same information for 8 September 2012. Bias values ranged from  $-4.66$   
24 to  $0.22$  dB, and did not show fluctuations due to low sample numbers.

25 Figure 11 shows a scatter plot of 1 hour radar rainfall, calculated using  $Z = 200 R^{1.6}$ , and  
26 gauge rainfall, for 25 August 2014 and 8 September 2012. The RMSE and NE of rainfall pairs  
27 on 25 August 2014 were improved from  $65.7$  to  $29.7$  mm and from  $0.79$  to  $0.31$ , respectively.  
28 On 8 September 2012, RMSE and NE were improved from  $30.0$  to  $21.8$  mm and from  $0.58$  to  
29  $0.40$ , respectively, by the use of bias correction, while CC was unchanged at  $0.81$ . Again, in  
30 both cases the use of corrected reflectivity for rainfall estimation was found to improve the  
31 accuracy compared with raw reflectivity.



### 1 **3.3 Disdrometer method**

2 Before using the disdrometer bias correction method to estimate rainfall rates, 10 min rain  
3 rates obtained directly from DSDs and from collocated gauges were compared. Figure 12  
4 shows the time series of rain rate obtained by PARSIVEL (red circles) and collocated gauges  
5 (blue circles) on 25 August 2014. Daily total rainfall amounts for PARSIVEL and the gauges  
6 were 129.4 and 116.0 mm, respectively. The difference in the totals is only 13.4 mm, and the  
7 RMSE and CC between the 10 min time series were  $0.52 \text{ mm h}^{-1}$  and 0.99, respectively. On 8  
8 September 2012 (not shown), the difference between the total daily rainfall amounts was 0.7  
9 mm and the RMSE and CC between the two 10 min series were  $0.62 \text{ mm h}^{-1}$  and 0.96,  
10 respectively. It is concluded that DSDs were sufficiently reliable to use as a reference with  
11 which to calculate the radar bias.

12 Figure 13 shows time series of reflectivity obtained by radar (black circles) and by  
13 PARSIVEL (red circles), and the radar bias (blue circles), on 25 August 2014. The bias was  
14 more stable before 1200 LST than after 1400 LST. PARSIVEL reflectivity fell to zero from  
15 1230 to 1340 LST because the precipitation system moved away from the PARSIVEL site.  
16 Because of this discontinuity, the bias can be considered to be reliable only until 1200 LST.

17 Figure 14 shows time series of reflectivity obtained by radar (black circles) and by  
18 PARSIVEL (red circles), and the radar bias (blue circles), on 8 September 2012. On this  
19 occasion there was no reflectivity data from either PARSIVEL or radar until 0330 LST.

20 Figure 15 shows a scatter plot of hourly radar rainfall, calculated using  $Z = 200 R^{1.6}$ , and  
21 gauge rainfall, on 25 August 2014 and 8 September 2012. The RMSE and NE of rainfall pairs  
22 on 25 August 2014 were improved from 65.7 mm to 42.0 mm and from 0.79 to 0.40,  
23 respectively. On 8 September 2012, RMSE and NE decreased from 30.1 to 24.6 mm, and  
24 from 0.58 to 0.46, respectively, while CC decreased from 0.81 to 0.65. In both cases, using  
25 corrected rather than raw reflectivity for rainfall estimation improved accuracy as measured  
26 by RMSE and NE, but reduced accuracy as measured by CC.

### 27 **3.4 Discussion**

28 Figure 16 shows hourly rainfall RMSE from each of the different bias correction methods on  
29 25 August 2014 and 8 September 2012. Red, black, green, and blue bars show the RMSE  
30 obtained using the uncorrected, equidistance line, overlapping area, and disdrometer methods,  
31 respectively. The disdrometer method produced the lowest RMSE before 1200 LST and the





1 highest RMSE after 1200 LST (Fig. 16a). This behavior can be attributed to the varying  
2 stability of the reflectivity calculated by PARSIVEL (Fig. 13). The overlapping method is  
3 more accurate than the equidistance line method for the entire time period, except at 1400  
4 LST. All the bias correction methods performed better than the uncorrected method, except  
5 for the period during which DSDs were unavailable. On 8 September 2012, the RMSE of the  
6 overlapping area method was lower than that of the other methods for the entire period,  
7 except at 0500 and 0600 LST (Fig. 16(b)). The disdrometer method produced lower RMSE at  
8 0600 LST, when DSDs were available, and the equidistance line method was more accurate at  
9 0500 LST, when the sample number was high (Fig. 13). Considering the entire period  
10 covering both events, the overlapping area method showed the best performance, as measured  
11 by RMSE. The accuracy of radar rainfall estimates could be improved by combining the three  
12 approaches, using metrics such as DSD temporal stability and the number of samples  
13 available for the equidistance line method to select the best method for a particular situation.

14

#### 15 **4 Conclusions**

16 Three methods for determining the reflectivity bias of single polarization radar using dual  
17 polarization radar reflectivity and disdrometer data were proposed and examined for two  
18 rainfall events caused by low pressure over the Korean Peninsula on 25 August 2014 and 8  
19 September 2012. Single polarization radar reflectivity was underestimated by more than 12  
20 dB and 7 dB during the August and September events, respectively. All three methods  
21 improved the accuracy of estimated rainfall, except during a period when DSDs were not  
22 observed (as the precipitation system did not pass over the disdrometer location). The use of  
23 these bias correction methods reduced rainfall RMSE by up to 50%. Overall, the accuracy of  
24 rainfall estimation was highest when the overlapping area method was used to correct radar  
25 reflectivity.

26 The reflectivity biases obtained using the disdrometer and equidistance line methods were  
27 more temporally variable than those obtained using the overlapping area method. There were  
28 several hours during which the disdrometer method was more accurate than the overlapping  
29 area method. We suggest that combining the overlapping area method with the disdrometer  
30 method, using threshold criteria such as the temporal stability of reflectivity and the number  
31 of samples available would allow more accurate estimates of rainfall. However, optimum  
32 values for the domain size for the overlapping area method, the sample number threshold for



1 the equidistance line method, and the reflectivity threshold for the disdrometer method should  
2 be determined in order to combine the three methods most effectively.

3

4

### 5 **Acknowledgements**

6 The authors thank the Ministry of Land, Infrastructure, and Transport of the Korean  
7 government and the Korean Meteorological Administration for providing radar data and AWS  
8 (Automatic Weather System) gauge data. This research was funded by the Korea  
9 Meteorological Industry Promotion Agency under Grant KMIPA 2015-1050. And this  
10 research was partly funded by the Korea Meteorological Industry Promotion Agency under  
11 Grant KMIPA 2015-1060

12



## 1 **References**

- 2 Austin, P. M.: Relation between measure radar reflectivity and surface rainfall, Monthly  
3 Weather Review, 115, 1053-1070, 1987.
- 4 Battan, L. J.: Radar Observations of the Atmosphere, The University of Chicago Press,  
5 Chicago and London, 324, 1973.
- 6 Campos, E. and Zawadzki, I.: “Instrumental uncertainties in Z-R relations”, Journal of  
7 Applied Meteorology, 36, 1088-1102, 2000.
- 8 Gorgucci E., Scarchilli G., and Chandrasekar V.: Calibration of radars using polarimetric  
9 techniques. IEEE Transactions on Geoscience and Remote Sensing, 30: 853-858, 1992.
- 10 Gorgucci, E., Scarchilli, G., and Chandrasekar, V.: A procedure to calibrate multiparameter  
11 weather radar using properties of the rain medium. IEEE Transactions on Geoscience and  
12 Remote Sensing, 37: 269–276, 1999.
- 13 Goddard J, Tan J, and Thurai M.: Technique for calibration of meteorological radars using  
14 differential phase. Electronic Letters, 30: 166 – 167, 1994.
- 15 Jang, M., Lee, D., and You, C.: Z-R relationship and DSD analyses using a POSS disdrometer.  
16 Part I: Precipitation cases in Busan, Journal of the Korean Meteorological Society, 40, 557-  
17 570, 2004.
- 18 Loffler-Mang, M. and Joss, J.: An optical disdrometer for measuring size and velocity of  
19 hydrometeors, J. Atmos. Oceanic. Technol., 17, 130-139, 2000.
- 20 Marks, D. A., Wolff, D. B., Carey, L. D., and Tokay, A.: Quality control and calibration of  
21 the dual-polarization radar at Kwajalein, RMI. Journal of Atmospheric and Oceanic  
22 Technology, 28: 181–196, 2011.
- 23 Rinehart, R. E.: Radar for meteorologists, fifth edition, Rinehart Publications, Nevada, United  
24 States, pp. 482, 2010.
- 25 Ryzhkov, A. V., Giangrande, S. E., Melnikov, V. M., and Schuur, T. J.: Calibration issues of  
26 dual-polarization radar measurements. Journal of Atmospheric and Oceanic Technology, 22:  
27 1138–1155, 2005.

28



- 1 Scarchilli G., Gorgucci E., Chandrasekar V., and Dobaie A.: Self-consistency of polarization  
2 diversity measurement of rainfall. *IEEE Transactions on Geoscience and Remote Sensing*, 34:  
3 22–26, 1996.
- 4 Trabal J. M., Chandrasekar V., Gorgucci, E. and McLaughlin D. J.: Differential reflectivity  
5 (ZDR) calibration for CASA radar network using properties of the observed medium,  
6 *Geoscience and Remote Sensing Symposium, 2009 IEEE International, IGARSS 2009*  
7 (Volume:2) II-960-II963, 2009.
- 8 Vivekanandan J, Zrníc D. S., Ellis S. M., Oye R., Ryzhkov A. V., and Straka J.: Cloud  
9 microphysics retrieval using S-band dual-polarization radar measurements. *Bulletin of the*  
10 *American Meteorological Society*, 80(3): 381-388, 1999.
- 11 Wilson, J. W. and Brandes, E. A.: Radar measurement of rainfall-A summary, *Bulletin of the*  
12 *American Meteorological Society*, 60, 1048-1058, 1979.
- 13 You, C., Lee, D., Jang, M., Seo, K., Kim, K., and Kim, B.: The characteristics of rain drop  
14 size distributions using a POSS in Busan area, *Journal of the Korean Meteorological Society*,  
15 40, 713-724, 2004.
- 16 You, C., Lee, D., Jang, M., Uyeda, H., Shinoda, T., and Kobayashi, F.: Characteristics of  
17 rainfall systems accompanied with Changma front at Chujado in Korea, *Asia-Pacific Journal*  
18 *of Atmospheric Sciences*, 46, 41-51, 2010.
- 19 You, C.-H., Lee, D.-I., and Kang, M.-Y.: Rainfall estimation using specific differential phase  
20 for the first operational polarimetric radar in Korea, *Advances in Meteorology*, vol. 2014,  
21 Article ID 41317, 10 pages, doi:10.1155/2014/413717, 2014.
- 22 You, C.-H. and Lee, D.-I.: Decadal variation in raindrop size distributions in Busan, Korea,  
23 *Advances in Meteorology*, vol. 2015, Article ID 329327, 8 pages, 2015,  
24 doi:10.1155/2015/329327, 2015.
- 25 Zhang, J., Wang S., Clarke B.: WSR-88D reflectivity quality control using horizontal and  
26 vertical reflectivity structure. Preprints, 11<sup>th</sup> Conf. on Aviation, Range and Aerospace  
27 Meteorology, Hyannis, MA, Amer. Metroer. Soc, CD-ROM, P5.4, 2004
- 28
- 29



1 Table 1. Rainfall events used for the analysis.

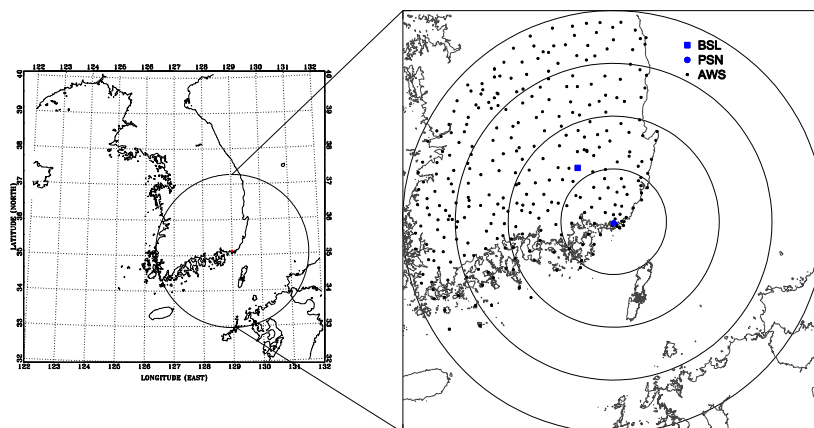
Date	Source	Period of analysis
8 September 2012	Low pressure	0000 LST to 0600 LST
25 August 2014	Low pressure	0900 LST to 1600 LST

2

3



1



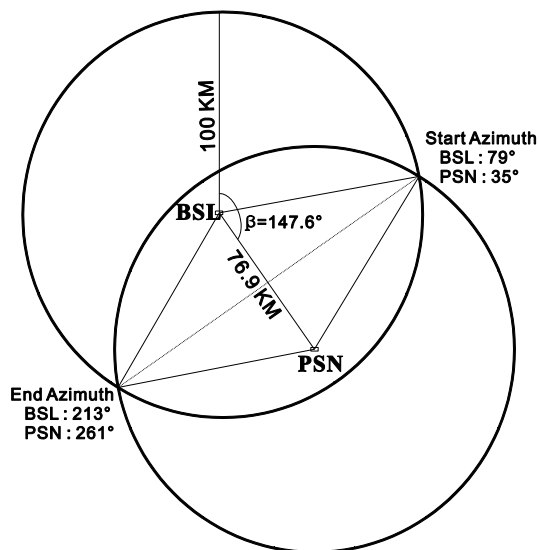
2

3 Figure 1. Location of the Bislsan radar (solid rectangle), the PARSIVEL disdrometer and  
4 Gudeok radar (solid circle), and rain gauges (black dots) distributed within 240 km of radar  
5 coverage. Circles indicate distance from the Gudeok radar, and are drawn at intervals of 60  
6 km.

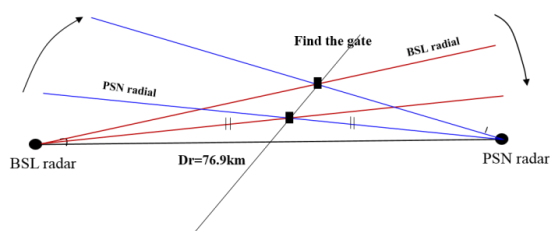
7



1



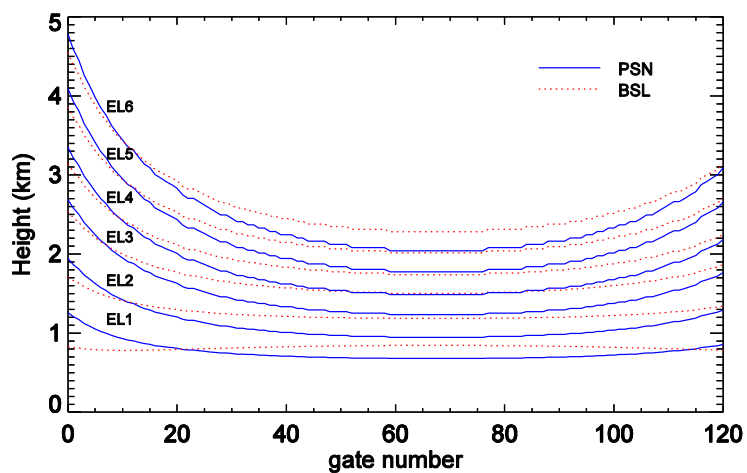
2



3

4

5 Figure 2. Schematic diagram showing the method used to calculate the line of equidistance  
6 between two radars. The effective radius was set to 100 km and the distance between radars is  
7 76.9 km. The azimuthal angle from BSL to PSN is 147.6 degrees. The start and end azimuthal  
8 angles are 79 (35) and 213 (261) degrees for BSL (PSN), respectively.



1

2 Figure 3. Beam height of PSN (blue solid lines) and BSL (red dotted lines) at the equidistance  
3 line. EL1 to EL6 show the lowest, second, third, fourth, fifth, and sixth elevation angles,  
4 respectively.

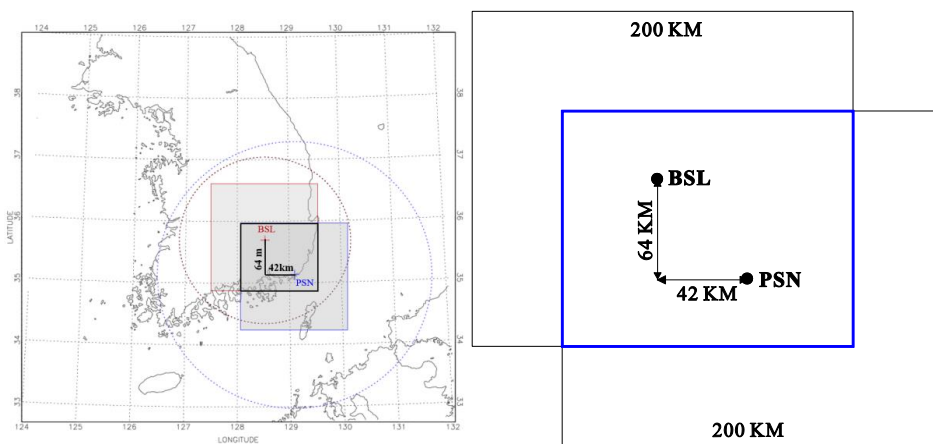
5





1

2



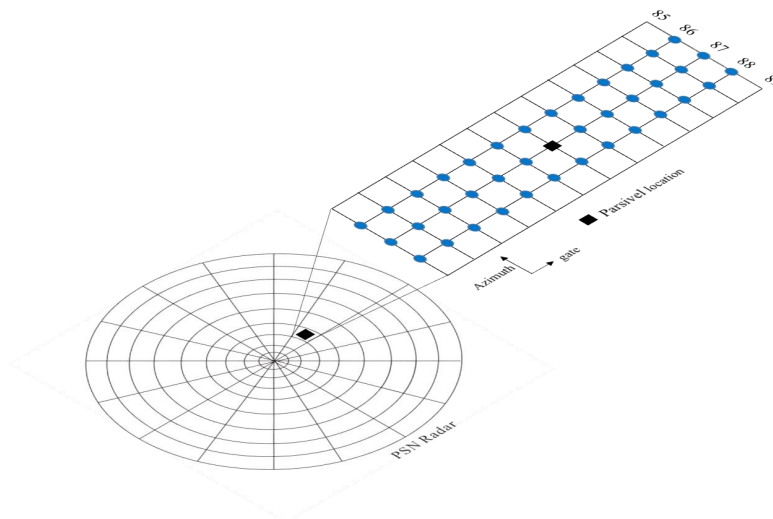
3

4 Figure 4. Schematic diagram of the overlapping area for BSL and PSN. The east–west and  
5 north–south distances between the two radars are 42 km and 64 km, respectively.

6



1



2

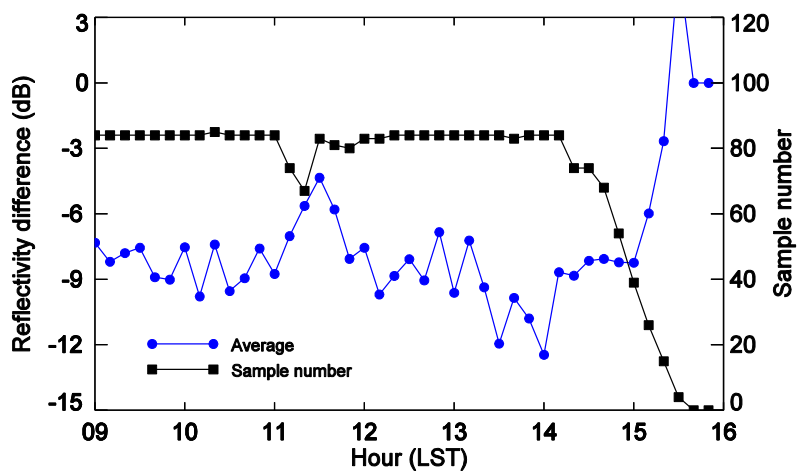
3 Figure 5. Schematic diagram showing matching of the radar gate and the PARSIVEL  
4 disdrometer. PARSIVEL is located ~9 km from the radar, at an azimuthal angle of 87 degrees.

5 The radar reflectivity was averaged over a  $3 \text{ km} \times 3^\circ$  domain centered at the PARSIVEL  
6 location.

7



1



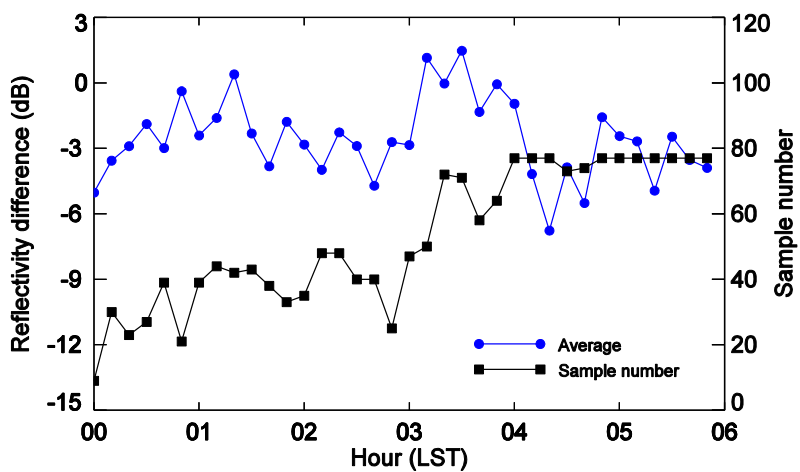
2

3 Figure 6. Time series of the average reflectivity difference between PSN and BSL at the  
4 equidistance line (blue circles) and the number of samples used in each calculation (black  
5 squares) on 25 August in 2014.

6



1



2

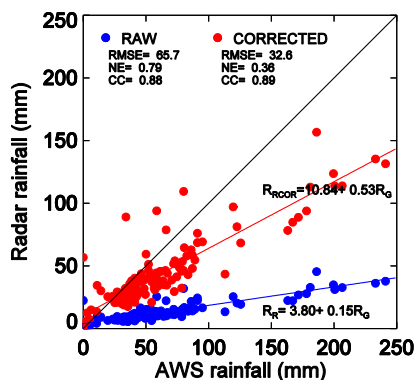
3 Figure 7. As for Fig. 6 but for 8 September 2012.

4

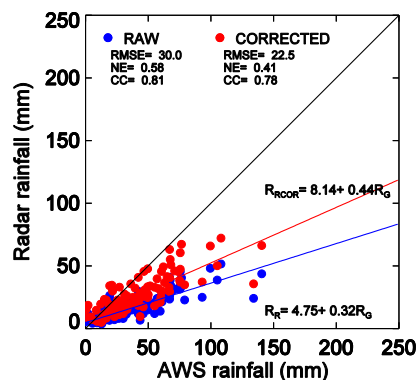


1

2 (a)



(b)



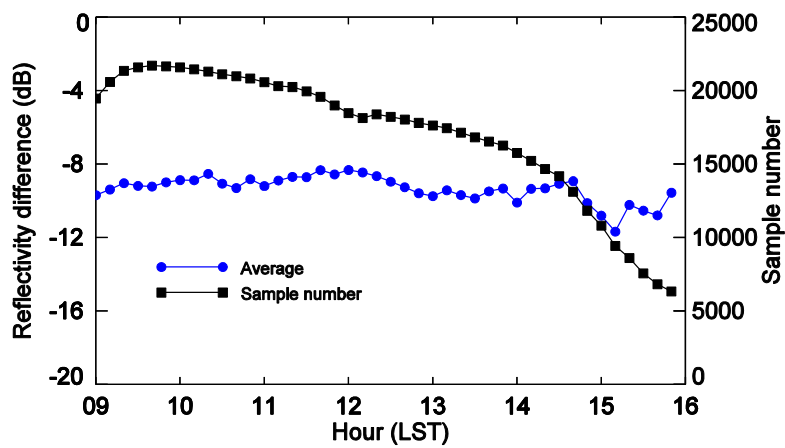
3

4 Figure 8. Scatter plot of hourly radar rainfall, calculated using  $Z = 200 R^{1.6}$ , and gauge rainfall,  
 5 for (a) 25 August 2014 and (b) 8 September 2012. Blue circles show the rainfall pairs  
 6 obtained using raw reflectivity and red circles show those obtained using reflectivity corrected  
 7 with the equidistance line method.

8



1



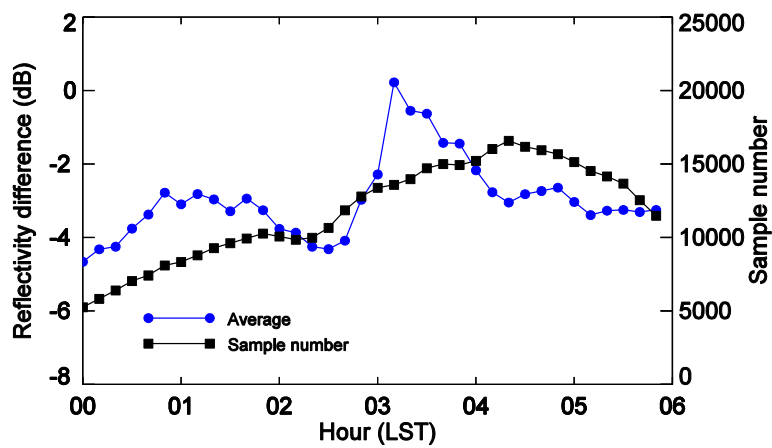
2

3 Figure 9. As for Fig. 6 but for the overlapping area method.

4



1



2

3 Figure 10. As for Fig. 7 but for the overlapping area method.

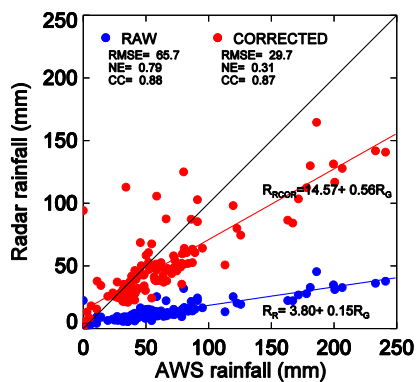
4



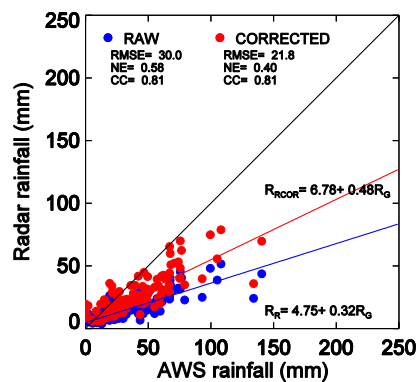
1

2

(a)



(b)



3

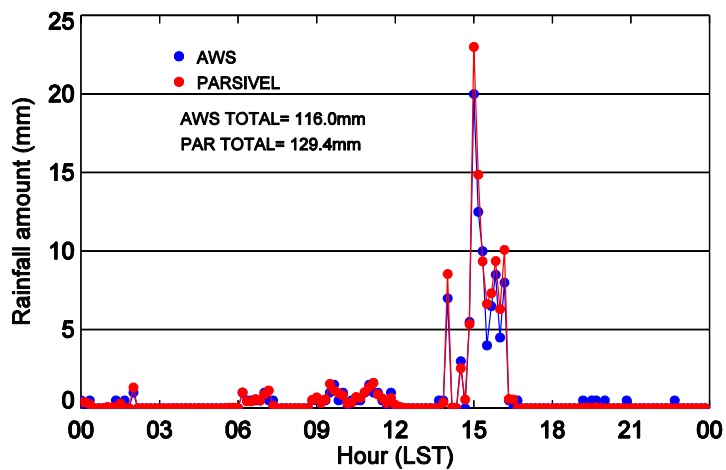
4 Figure 11. As for Fig. 8 but for the overlapping area method.

5





1



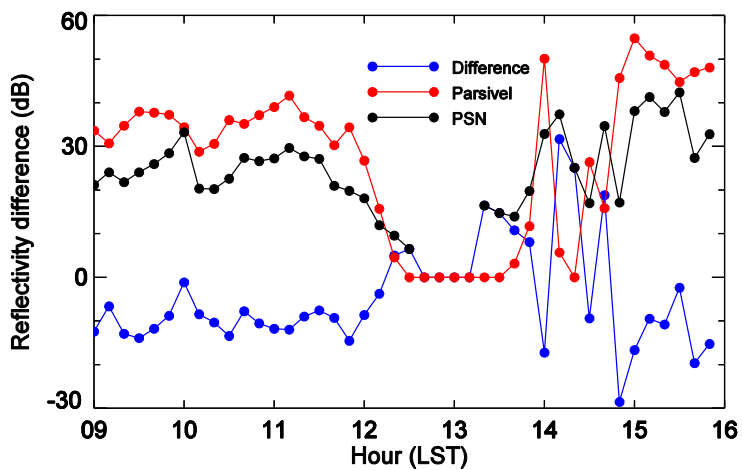
2

3 Figure 12. Time series of 10 min rainfall amount as obtained by PARSIVEL (red circles) and  
4 collocated gauges (blue circles).

5



1



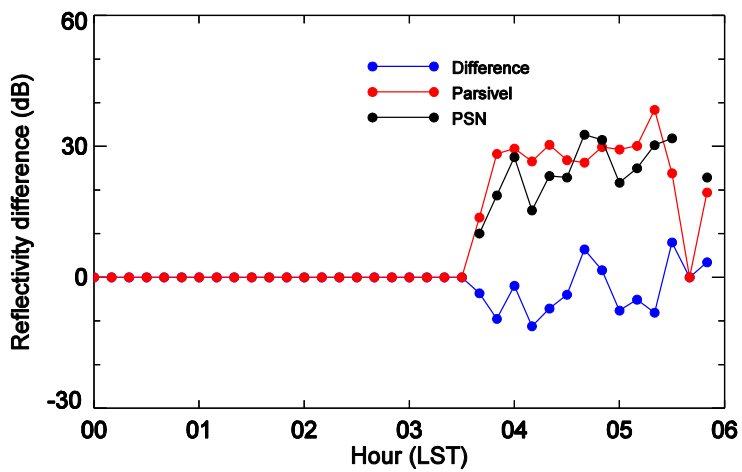
2

3 Figure 13. Time series of reflectivity obtained by radar (black circles) and by PARSIVEL (red  
4 circles), and the radar bias (blue circles) on 25 August 2014.

5



1



2

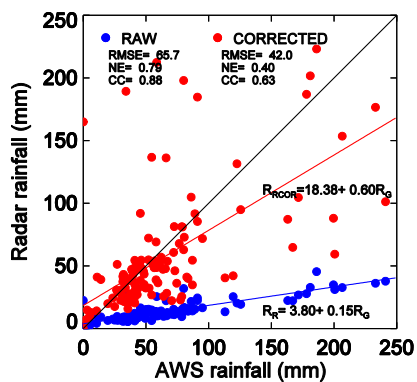
3 Figure 14. As for Fig. 13 but for 8 September 2012.

4

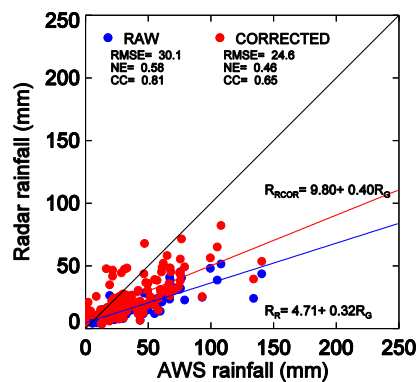


1

2 (a)



(b)



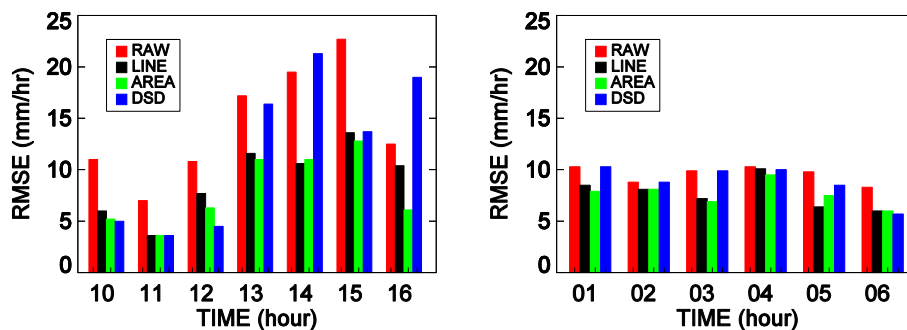
3

4 Figure 15. As for Fig. 8 but for the disdrometer method.

5



1



2

3 Figure 16. Hourly rainfall RMSE for different bias correction methods on 25 August 2014  
4 (left) and 8 September 2012 (right). The bars with different colors show results obtained using  
5 the raw data, equidistance line method, overlapping area method, and disdrometer method,  
6 respectively.

7